Modeling pressure transients in viscoelastic pipes

H.A. Warda, H.A. Kandil, A.A. Elmiligui and E.M. Wahba
Mechanical Engineering Dept., Faculty of Eng., Alexandria University, Alexandria, 21544, Egypt

In this study, a numerical model based on the Method of Characteristics (MOC) is developed for modeling pressure transients in viscoelastic pipes. The model is capable of dealing with unsteady friction and viscoelastic behavior of the pipe walls. These complex phenomena cause strong distortion of the pressure waves traveling through fluids that may not be predicted by the standard MOC. A universal model, developed by the authors, for unsteady friction for both laminar and turbulent flows is used in the analysis. The viscoelastic behavior of the pipe wall is modeled through a one element Kelvin-Voigt viscoelastic model that is in good agreement with the experimental data. The viscoelastic effect was shown to be the dominant damping factor of the pressure oscillations in transient flows through pipes exhibiting a viscoelastic behavior. The analysis showed also that unsteady friction has a minor effect on the damping of the pressure transient in viscoelastic pipes while it has a dominant damping effect in case of elastic pipes. An experimental setup was constructed to provide reliable experimental data for transient flows in PVC (viscoelastic) pipes to verify the numerical model. Eventually, the numerical model was experimentally verified to be capable of accurately and efficiently reproducing the experimentally measured pressure oscillations in viscoelastic pipes.

في هذه الدراسة تم تطوير نموذج رقمي معدل يعتمد على طريقة الخصائص ليكون قادرا على محاكاة الضغوط العابرة في المواسير ذات المرونة اللزجة. وهذا النموذج قادر على التعامل مع الظواهر المعقدة مثل الاحتكاك غير المستقر ومحاكاة سلوك جدران المواسير ذات المرونة اللزجة. هذه الظواهر تؤدى إلى عدم قدرة طريقة الخصائص البسيطة على محاكاة الموجات التضاغطية التي تتولد في المواسير خاصة بعد مرور الموجة التضاغطية الأولى حيث لا تتضمن طريقة الخصائص البسيطة نماذج رياضية دقيقة لمحاكاة هذه الظواهر ومن ثم زادت الحاجة لتطوير طريقة الخصائص البسيطة. بالنسبة للاحتكاك غير المستقر في المواسير فقد تمت محاكاته باستخدام نموذج عام تم تطويره بواسطة مؤلفي هذا البحث ونشر فى بحث سابق. وهذا النموذج قادر على محاكاة الاحتكاك غير المستقر في جميع أطوار السريان. وقد أوضح التحليل أن الاحتكاك غير المستقر هو السبب الرئيسي لتضاؤل الموجات التضاغطية في المواسير المرنة ولكن تأثيره مهمل على تضاؤل الموجات التضاغطية في المواسير ذات المرونة اللزجة. تمت محاكاة المرونة اللزجة للمواسير من خلال نموذج كيلفن – فويجت ذو عنصر واحد ونجح هذا النموذج في إعطاء نتائج متوافقة مع النتائج المعملية وتم توضيح تأثير المرونة للمواسير على السريان العابر. ثم أيضا توضح أن المرونة اللزجة للمواسير هي العامل الرئيسي المؤثر على تضاؤل الموجات التضاغطية في المواسير ذات المرونة اللزجة. أشارت النتائج أيضا إلي أهمية تقدير قيمة خواص المرونة اللزجة للمواسير المستخدمة في الصناعة. تم إنشاء جهاز معملي قادر على توفير نتائج معملية دقيقة للسريان العابر في المواسير ذات المرونة اللزجة للتحقق من صحة النموذج الرقمي الذي تم تطويره. وبالتالي تم التحقق من قدرة النموذج الرقمي المعدل لطريقة الخصائص على محاكاة السريان العابر في المواسير آخذا في الاعتبار تأثير الظواهر السابق ذكرها.

Keywords: Viscoelastic pipes, Unsteady friction, Pressure transients

1. Introduction

This study is concerned with studying the pressure transient propagation within fluids flowing in viscoelastic pipes. The viscoelastic behavior of the pipe walls was studied thoroughly to eliminate the discrepancy between the experimental data and the results predicted numerically using the standard MOC.

The MOC is a general mathematical technique that can be used for solving a pair of quasi-linear hyperbolic partial differential equations. The equations describing the pressure-transient wave propagation through fluid flows in pipes belong to this family of problems. This method was first proposed by Rieman in 1860. By the early 1970s, the method was established as the standard method for transient analysis. Studies covering the application of the MOC to transient problems such as water hammer problems developed continuously over the last 50 years.

Watters [1] provided the detailed theoretical basis for estimating the wave speed in different types of pipes. Also, Wylie and Streeter [2] summarized the various methods of solution for the water hammer problem. They stated that the MOC is considered to be the standard numerical method by which other methods may be judged, for accuracy and efficiency, for pressure transients. Also, Kaplan et al. [3] showed that transients arising in long oil pipelines could be adequately simulated by the MOC.

A noticeable distortion was observed between the experimental data and the results of the numerical models based on the standard MOC. This problem attracted several researchers to enhance the modeling of unsteady friction together with accounting for the additional damping due to viscoelastic behavior of the pipe wall.

For example, Zielke [4] developed a weighting-function model, for friction losses in transient laminar pipe flow, based on an exact analytical solution of laminar flow equations. Later, Zielke's model was greatly modified by Trikha [5]. Also, Suzuki et al. [6] presented an alternative approach for improving Zielke's weighting function model for laminar flow. Vardy et al. [7, 8] developed a weighting function model for transient turbulent pipe friction at moderate Reynolds numbers ($< 10^5$) in a manner similar to Zielke's expression for laminar flows. Another weighting-function model for transient turbulent friction in smooth pipes was developed by Vardy and Brown [9].

Another unsteady-friction model was developed by Brunone et al. [10, 11] for turbulent flows in the form of an additional term to the momentum equation. Brunone et al. [12] introduced a modified characteristics method where they applied the usual equations of the MOC and evaluated the new added term in an explicit manner.

Recently, the above mentioned unsteady friction models were tested by Warda et al. [13] for both laminar and turbulent flow cases. They concluded that none of the available models could be used accurately and efficiently for both laminar and turbulent flows. A universal model was developed by introducing a modification to Vardy et al.'s model originally developed for turbulent flow. The modified model was experimentally verified [13] to be capable of modeling unsteady friction in elastic pipes while some differences were observed for viscoelastic pipes.

The methods of studying viscoelastic effects may be divided into two categories; one is based on the MOC while the other is based on frequency-response method. According to Suo and Wylie [14], Rieutord and Blanchard (1979) applied the MOC to study the effect of the viscoelastic behavior of the pipe walls on the transients. Gally, Guney and Rieutord (1979) compared the calculated water hammer in polyethylene pipes with laboratory test data, showing a good agreement between numerical and experimental results. Guney [15] addressed the problem of water hammer created by closing a valve at the downstream end of a viscoelastic pipe. He proposed a modified MOC model that takes into account the effects of time-varying diameter and thickness. However, the model does not include any modeling for unsteady friction in case of turbulent flow and it was not verified against turbulent flow experimental data.

Pezzinga and Scandura [16] presented a theoretical and experimental study on the reduction of unsteady flow oscillations by using additional pipes of high-density polyethylene (HDPE), inserted at the upstream end of the pipeline, in a pumping installation. The mechanical behavior of the HDPE is described by both a linear elastic model and a Kelvin-Voigt viscoelastic model. The results of the mathematical model were in good agreement with the experimental data, even with only one Kelvin-Voigt element.

Warda et al. [13] studied the water hammer problem in elastic and viscoelastic pipes in the presence of unsteady friction. They used a universal model for unsteady friction that can be used for both laminar and turbulent flows. The model gave excellent results with elastic pipes. However, there was a noticeable difference between the results of the model and the experimental measurements in the case of PVC pipes. Therefore, the numerical model has to be modified to account for the viscoelastic effects of the pipe wall.

From the previous review, it is noted that no modified MOC has been verified experimentally to be capable of handling water

hammer problems in viscoelastic (PVC) pipes in the presence of unsteady friction. Therefore, the model developed in this study has to overcome the drawbacks of previous studies. To achieve this goal, the following steps are performed:

1) An unsteady friction model capable of accurately simulating unsteady friction for laminar and turbulent flows is used in the analysis.

2) The MOC is modified to account for the viscoelastic effects of the pipe wall.

3) Extensive experimental work was performed to produce reliable experimental data for testing and verifying the numerical model.

2. Experimental analysis

2.1. Experimental setup

An experimental setup was constructed in the Fluid Mechanics Laboratory at the Faculty of Engineering, Alexandria University for providing reliable experimental data for verifying the numerical model. The setup is schematically shown in fig. 1. The setup consists of the following main parts:

1) A constant-head tank of 9-cubic-meter-capacity installed on the roof of the laboratory. The tank holds a maximum head of 11 meters above the test-pipe centerline. A centrifugal pump continuously feeds the tank with water to maintain a constant free-surface level. The tank is connected via a 10-cm-diameter vertical pipe to a pressurized tank (ground tank) of 0.2 cubic meters capacity.

2) A PVC pipe of 25.4-mm inside diameter, 4.2-mm thickness and 25.6-m. length. The water flow rate through the PVC pipe could be controlled using a gate valve. The flow rate is measured using a calibrated tank and a stopwatch.

3) A normally closed solenoid-operated valve with a closure time of 0.08 seconds.

4) Measuring, monitoring and recording equipment that include: two piezoelectric pressure transducers mounted on the PVC pipe at locations 0.03 m and 15.3 m upstream of the solenoid valve. Each transducer is connected to a one-channel charge amplifier (Type 5011). The charge amplifier is responsible for converting the electric charge produced by the piezoelectric transducer into a proportional voltage signal.

The output signal from the charge amplifier is transmitted to a LeCroy (Type 6810) waveform recorder that converts analog waveforms into digital data. The signal recorded by the waveform recorder is then transferred to a personal computer through a GPIB interface card. Software packages are then used to display and analyze the recorded pressure data.

2.2. Experimental test cases

The test cases performed using a test pipe of a length of 25.6 m, an inside diameters of 0.0254 m and a wall thickness of 0.0042 m, are summarized in the following table.

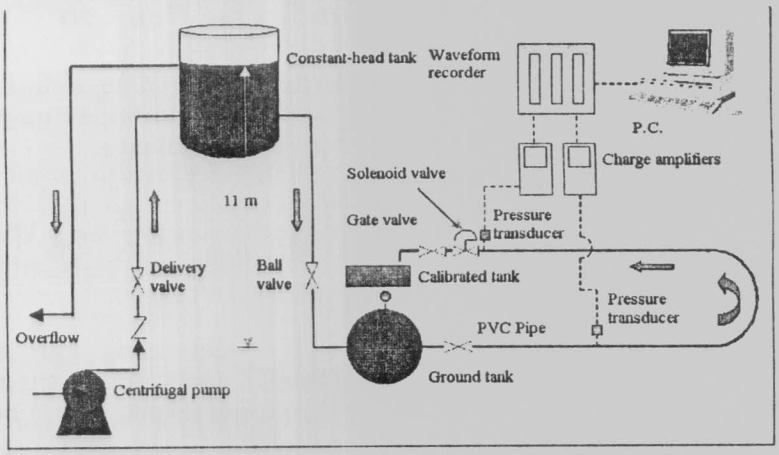

Fig. 1. Diagrammatic sketch of the experimental setup.

Test case no.	1	2	3	4	5
Steady state velocity, V_o (m/s)	0.062	0.233	0.285	2.2695	0.0235
Reynolds Number, R_N	1575	5918	7239	57645	597
Coefficient of friction, f	0.04	0.035	0.032	0.03	0.107

In test cases (1, 2, 3, and 4) measurements were taken at the solenoid valve only. In test case (5) measurements were taken at both the valve and a point 15.3-m upstream of the valve.

2.3. Measurement of the wave speed

The wave speed was measured by initiating a transient and recording two pressure signals through the two transducers and measuring the differential time between the start of the transient in both signals. By knowing the distance between the two transducers, the wave speed "a" (The ratio of distance between the two transducers to the differential time between the start of the transient in both signals) could be calculated

The previous procedure was applied to a laminar flow case with a velocity of 0.071 m/s (R_N=1803), and a turbulent flow case with a Reynolds number of 57645, as shown in figs. 2 and 3. In both cases the differential time between the two signals was found as 0.0295 seconds, which means a wave speed of 518 m/s.

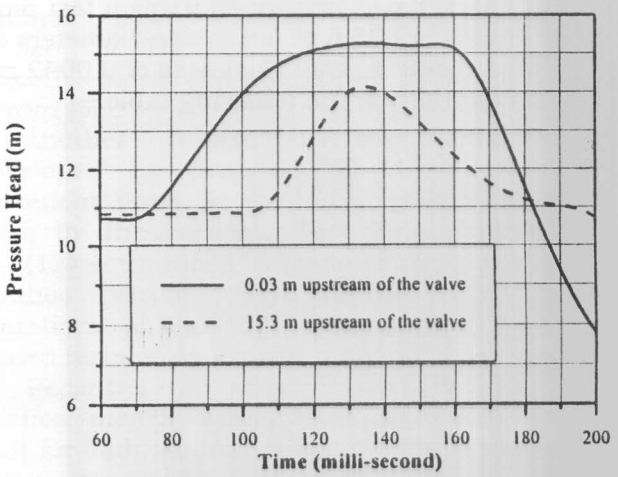

Fig. 2 Wave speed measurement for laminar flow data, R_N = 1803.

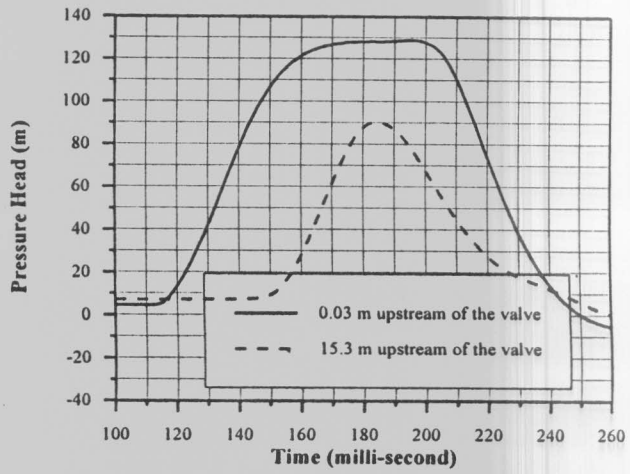

Fig. 3. Wave speed measurement from turbulent flow data, R_N = 57645.

3. Standard method of characteristics

The governing equations are given in Watters [1] as follows:
Continuity equation:

$$\frac{1}{\rho}\frac{dP}{dt} + a^2 \frac{\partial V}{\partial s} = 0 . \qquad (1)$$

Euler (Momentum) Equation:

$$\frac{dV}{dt} + \frac{1}{\rho}\frac{\partial P}{\partial s} + g\frac{dz}{ds} + \frac{f}{2D}V|V| = 0 . \qquad (2)$$

Introducing (λ) as a linear scale factor, the governing equations may be combined in one equation as follows:

$$\lambda\left(\frac{dV}{dt} + \frac{1}{\rho}\frac{\partial P}{\partial s} + g\frac{dz}{ds} + \frac{f}{2D}V|V|\right) + a^2\frac{\partial V}{\partial s} + \frac{1}{\rho}\frac{dP}{dt} = 0. \qquad (3)$$

By expanding the terms (dV/dt) and (dP/dt) down into their components and regrouping terms, eq. (3) becomes:

$$\left(\lambda\frac{\partial V}{\partial t}+(\lambda V+a^2)\frac{\partial V}{\partial s}\right)+\left(\frac{1}{\rho}\frac{\partial P}{\partial t}+(\frac{V}{\rho}+\frac{\lambda}{\rho})\frac{\partial P}{\partial s}\right)$$

$$+\lambda g\frac{dz}{ds}+\frac{\lambda f}{2D}V|V|=0. \qquad (4)$$

Some manipulations are then performed to this equation to replace the original two partial differential equations with two ordinary differential equations as follows:

$$\frac{dV}{dt}+\frac{g}{a}\frac{dH}{dt}-\frac{g}{a}V\frac{dz}{ds}+\frac{f}{2D}V|V|=0,$$

$$\text{for}\quad \frac{ds}{dt}=V+a, \qquad (5)$$

and,

$$\frac{dV}{dt}-\frac{g}{a}\frac{dH}{dt}+\frac{g}{a}V\frac{dz}{ds}+\frac{f}{2D}V|V|=0,$$

$$\text{for}\quad \frac{ds}{dt}=V-a \qquad (6)$$

Where the pressure (P) was replaced by its equivalent term $\rho g(H-z)$.

Eq. (5) is usually known as the C^+ characteristic equation while eq. (6) is known as the C^- characteristic equation. Eqs. (5) and (6) can now be expressed in a finite difference form, as follows:

The C^+ equation becomes

$$\frac{V_P-V_L}{\Delta t}+\frac{g}{a}\frac{H_P-H_L}{\Delta t}-\frac{g}{a}V_L\frac{dz}{ds}+\frac{fV_L|V_L|}{2D}=0. \qquad (7)$$

The C^- equation becomes

$$\frac{V_P-V_R}{\Delta t}-\frac{g}{a}\frac{H_P-H_R}{\Delta t}+\frac{g}{a}V_R\frac{dz}{ds}+\frac{fV_R|V_R|}{2D}=0. \qquad (8)$$

To apply the finite difference numerical technique, the pipe has to be divided into a number of sections. Grid points along the s-axis represent points that are spaced by (Δs) along the pipe.

4. Viscoelastic materials

Viscoelasticity describes a property of the material that simultaneously exhibits a combination of viscous and elastic behaviors. When a sudden load is applied to a viscoelastic material, there is an initial rapid extension and the material continues to extend with time; this phenomena is well known as creep. When the load is removed, there is an initial rapid contraction that quickly slows down. Conversely, the stress required to maintain constant strain decreases with time. This is known as stress relaxation.

A common approach to modeling viscoelastic behavior is by means of combining elements representing ideal elastic behavior and ideal viscous behavior. This can be done by using springs representing ideal elastic properties and a dashpot representing ideal viscous properties.

4.1. Modeling of pipes exhibiting a linear viscoelastic behavior

If the pipe material exhibits a linear viscoelastic behavior, then a Kelvin-Voigt model [8] can be adopted to simulate this phenomenon. A Kelvin-Voigt model is represented by a series of elements, the first element is a simple spring that represents the instantaneous strain component and the other elements comprise a spring combined in parallel with a viscous damping mechanism (dash-pot) and represent the retarded strain component.

The total strain can be expressed by summing the instantaneous and retarded strain components:

$$\varepsilon=\varepsilon_I+\varepsilon_R. \qquad (9)$$

Where, ε is the strain in pipe wall, ε_I is the instantaneous strain, and ε_R is the retarded strain. Using a Kelvin-Voigt model with (n) elements, the retarded strain could be expressed as:

$$\varepsilon_R=\sum_{j=1}^{n}\varepsilon_j. \qquad (10)$$

Where, ε_j is the strain of the j^{th} Kelvin-Voigt element.

The instantaneous strain component can be expressed as:

$$\varepsilon_I = \frac{\sigma}{E_o}. \qquad (11)$$

Where, E_o is the Modulus of Elasticity for the instantaneous strain, and σ is the stress at the pipe wall. The retarded strain component can be obtained from the following differential equation:

$$\sigma = E_j \varepsilon_j + \eta_j \frac{d\varepsilon_j}{dt}. \qquad (12)$$

Where, η_j is the viscosity of the generic element and E_j is the modulus of elasticity of the generic element. This equation can be written in the following equivalent form:

$$\frac{d\varepsilon_j}{dt} = \frac{1}{\tau_j}\left(\frac{\sigma}{E_j} - \varepsilon_j\right). \qquad (13)$$

Where, $\tau_j = \frac{\eta_j}{E_j}$ is the retardation time of the j^{th} Kelvin-Voigt element.

When the pipe is subjected to the internal pressure (p), one can get the following equations:

$$\varepsilon_I = \frac{pD\ \lambda}{2\ eE_o}, \text{ and} \qquad (14)$$

$$\frac{d\varepsilon_j}{dt} = \frac{1}{\tau_j}\left(\frac{pD\lambda}{2eE_j} - \varepsilon_j\right). \qquad (15)$$

Where, D is the pipe diameter, e is the pipe wall thickness and λ is the constraint coefficient in the wave-speed formula.

The introduction of the linear viscoelastic behavior of the pipe walls modifies only the continuity equation.

4.2. The modified continuity equation

A control volume coinciding with the interior of the pipe and of length (ds), as shown in fig. 4 is considered for deriving the modified continuity equation.

Conservation of mass gives:

$$\rho Q - \left(\rho Q + \frac{\partial}{\partial s}(\rho Q)ds\right) = \frac{\partial}{\partial t}(\rho A ds),$$

which is simplified to the following form:

$$-\frac{\partial}{\partial s}(\rho Q)ds = \frac{\partial}{\partial t}(\rho A ds).$$

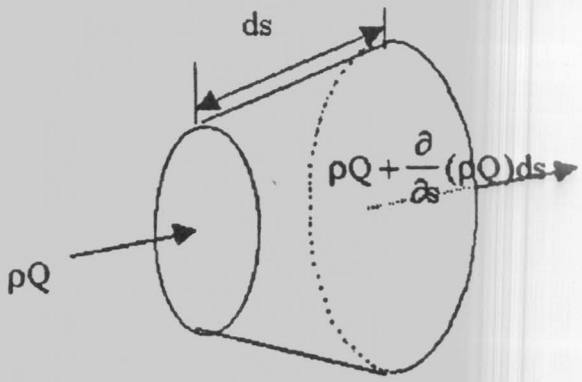

Fig. 4. Control volume for deriving the continuity equation

The ends of the control volume are allowed to move longitudinally with the pipe as it stretches. This concept is employed because the pipe stretching affects the available storage volume.

Now, by expanding the parentheses, the equation becomes:

$$-\rho\frac{\partial Q}{\partial s}ds - Q\frac{\partial \rho}{\partial s}ds = \rho A\frac{\partial}{\partial t}(ds) + \rho ds\frac{\partial A}{\partial t} + Ads\frac{\partial \rho}{\partial t}.$$

Regrouping and dividing by (ρAds) give,

$$\frac{1}{\rho}\left(\frac{\partial \rho}{\partial t} + V\frac{\partial \rho}{\partial s}\right) + \frac{1}{A}\frac{\partial A}{\partial t} + \frac{1}{A}\frac{\partial Q}{\partial s} + \frac{1}{ds}\frac{\partial}{\partial t}(ds) = 0.$$

Since (*ds*) is fixed to the pipe walls, therefore it varies only with time then the continuity equation could be further simplified to:

$$\frac{1}{\rho}\frac{d\rho}{dt} + \frac{1}{A}\frac{\partial A}{\partial t} + \frac{1}{A}\frac{\partial Q}{\partial s} + \frac{1}{ds}\frac{d}{dt}(ds) = 0. \qquad (16)$$

To express the density and area terms in terms of pressure, the Bulk Modulus of Elasticity of the fluid, $K = \frac{dP}{\frac{d\rho}{\rho}}$, is introduced in the form:

$$\frac{1}{\rho}\frac{d\rho}{dt} = \frac{1}{K}\frac{dP}{dt} \quad . \tag{17}$$

To develop an expression for $(\partial A/\partial t)$, in terms of pressure, in eq. (16), consider the stretching of the cross-sectional area (A), where $A = \frac{\pi}{4} D^2 (1+\varepsilon)^2$, differentiating w.r.t. time gives:

$$\frac{\partial A}{\partial t} = \frac{\pi}{4} D^2 2 \frac{\partial \varepsilon}{\partial t} . \tag{18}$$

The modification of the viscoelastic behavior of the pipe wall will now be introduced through the temporal partial derivative of the circumferential strain by substituting eq. (9) into eq. (18) as follows:

$$\frac{\partial A}{\partial t} = \frac{\pi}{2} D^2 \left(\frac{\partial \varepsilon_I}{\partial t} + \frac{\partial \varepsilon_R}{\partial t} \right) .$$

And from eq. (13), one gets:

$$\frac{\partial A}{\partial t} = \frac{\pi}{2} D^2 \left(\frac{D\lambda}{2eE_o} \frac{\partial P}{\partial t} + \frac{\partial \varepsilon_R}{\partial t} \right) .$$

By assuming that $(1+\varepsilon) \approx 1$ and dividing by the cross-sectional area (A), one gets:

$$\frac{1}{A}\frac{\partial A}{\partial t} = 2\left(\frac{D\lambda}{2eE_o} \frac{\partial P}{\partial t} + \frac{\partial \varepsilon_R}{\partial t} \right) . \tag{19}$$

As stated by Watters [1], the restraint type would not affect the end result for the continuity equation. Wylie and Streeter [2] stated that the type of restraint is taken into account only through the factor (λ) in the wave speed formula.

Hence, when evaluating the term $\left(\frac{1}{ds}\frac{d}{dt}(ds)\right)$ in eq. (16), the simple restraint case of $(d\varepsilon_{long} = 0)$, where (ε_{long}) is the longitudinal strain could be applied,

$$d(ds) = d\varepsilon_{long}\, ds = 0,$$

$$\frac{1}{ds}\frac{d}{dt}(ds) = 0 . \tag{20}$$

Now, by substituting eqs. (17), (19), and (20) into eq. (16), the following equation. is obtained:

$$\frac{1}{K}\frac{dP}{dt} + \frac{D\lambda}{eE_o}\frac{\partial P}{\partial t} + 2\frac{\partial \varepsilon_R}{\partial t} + \frac{1}{A}\frac{\partial Q}{\partial s} = 0 .$$

Neglecting the spatial derivative for the pressure with respect to the temporal derivative, the equation becomes:

$$\left(\frac{1}{K} + \frac{D\lambda}{eE_o}\right)\frac{\partial P}{\partial t} + 2\frac{\partial \varepsilon_R}{\partial t} + \frac{1}{A}\frac{\partial Q}{\partial s} = 0 .$$

Taking into consideration the equation for the wave speed given by Watters [1], in the form:

$$\frac{1}{K} + \frac{D\lambda}{eE_o} = \frac{1}{\rho a^2} ,$$ the continuity equation is

reduced to the following form:

$$\frac{1}{\rho a^2}\frac{\partial P}{\partial t} + 2\frac{\partial \varepsilon_R}{\partial t} + \frac{1}{A}\frac{\partial Q}{\partial s} = 0 . \tag{21}$$

By replacing the pressure term (P) with the piezometric head (H) and utilizing eq. (9), eq. (21) becomes:

$$\frac{\partial H}{\partial t} + \frac{a^2}{gA}\frac{\partial Q}{\partial s} + 2\frac{a^2}{g}\sum_{j=1}^{n}\frac{\partial \varepsilon_j}{\partial t} = 0 .$$

An equivalent form could be reached following the above procedure if the velocity (V) is considered to be the dependent variable instead of the flow rate (Q),

$$\frac{dH}{dt}+\frac{a^2}{g}\frac{\partial V}{\partial s}+2\frac{a^2}{g}\sum_{j=1}^{n}\frac{d\varepsilon_j}{dt}=0\,.$$

For simplicity, a Kelvin-Voigt model with only one element will be assumed and the continuity equation will take the following form:

$$\frac{dH}{dt}+\frac{a^2}{g}\frac{\partial V}{\partial s}+2\frac{a^2}{g}\frac{d\varepsilon_1}{dt}=0\,. \qquad (22)$$

From eq. (14) and by substituting a value of j=1 for the Kelvin-Voigt element, the equation takes the following form:

$$\frac{d\varepsilon_1}{dt}=\frac{1}{\tau_1}\left(\frac{PD\lambda}{2eE_1}-\varepsilon_1\right). \qquad (23)$$

By substituting from eq. (23) into eq. (22), one gets:

$$\frac{dH}{dt}+\frac{a^2}{g}\frac{\partial V}{\partial s}+2\frac{a^2}{g}\frac{1}{\tau_1}\left(\frac{PD\lambda}{2eE_1}-\varepsilon_1\right)=0\,. \qquad (24)$$

Hence, an additional term appeared in the continuity equation to account for the viscoelastic behavior of the pipe walls as given in eq. (24).

4.3. The modified MOC model

When eq. (24) is solved with the momentum equation by the method of characteristics, following the same procedure in section (3), the following characteristic equations are obtained in which the dominant effect of this viscoelastic nature is clearly recognized.

$$C^+: V_P-V_L+\frac{g}{a}(H_P-H_L)-\frac{g\Delta t}{a}V_L\frac{dz}{ds}+gh_{fL}\Delta t+\frac{2a\Delta t}{\tau_1}\left(\frac{\rho gH_L D\lambda}{2eE_1}-\varepsilon_{1L}{}^{t-\Delta t}\right)=0. \qquad (25)$$

$$C^-: V_P-V_R-\frac{g}{a}(H_P-H_R)+\frac{g\Delta t}{a}V_R\frac{dz}{ds}+gh_{fR}\Delta t+\frac{2a\Delta t}{\tau_1}\left(\frac{\rho gH_R D\lambda}{2eE_1}-\varepsilon_{1R}{}^{t-\Delta t}\right)=0\,. \qquad (26)$$

The values of the retarded strain $\varepsilon_{1L}{}^{t}$ and $\varepsilon_{1R}{}^{t}$ could be computed at each time step from the following equations, obtained from eq. (23):

$$\frac{\varepsilon_{1L}{}^{t}-\varepsilon_{1L}{}^{t-\Delta t}}{dt}=\frac{1}{\tau_1}\left(\frac{\rho gH_L D\lambda}{2eE_1}-\varepsilon_{1L}{}^{t-\Delta t}\right), \qquad (27)$$

and

$$\frac{\varepsilon_{1R}{}^{t}-\varepsilon_{1R}{}^{t-\Delta t}}{dt}=\frac{1}{\tau_1}\left(\frac{\rho gH_R D\lambda}{2eE_1}-\varepsilon_{1R}{}^{t-\Delta t}\right). \qquad (28)$$

It was shown by Warda et Al. [7] that the unsteady friction terms (h_{fL} and h_{fR}) are accurately modeled by Vardy et al.`s friction model. Vardy et al.`s model is suitable for turbulent flows, while an adjustment was introduced for laminar flows. The equations for Vardy et al.`s friction model are given by:

$$h_{fL}(K\Delta t)=\frac{fV_L(i,K\Delta t)|V_L(i,K\Delta t)|}{4gR}+\frac{4\nu}{gR^2}\sum_{J=1}^{K}[V_L((i,K-J+1)\Delta t)-V_L((i,K-J)\Delta t)]\,W\left[\left(J-\frac{1}{2}\right)\Delta t\right], \qquad (29)$$

$$h_{fR}(K\Delta t)=\frac{fV_R(i,K\Delta t)|V_R(i,K\Delta t)|}{4gR}+\frac{4\nu}{gR^2}\sum_{J=1}^{K}[V_R((i,K-J+1)\Delta t)-V_R((i,K-J)\Delta t)]\,W\left[\left(J-\frac{1}{2}\right)\Delta t\right], \text{ and} \qquad (30)$$

$$W(t)=\overline{W}(\tau)=\left(\frac{1}{2\sqrt{\pi\tau}}\right)e^{-\tau/C^*}. \qquad (31)$$

Where,

$\tau = \frac{\nu}{R^2} t$ = dimensionless time and

C* is the shear decay coefficient = $\frac{7.41}{R_N{}^b}$ (32)

The exponent, b is given by:

$$b = \log_{10}\left(\frac{14.3}{R_N{}^{0.05}}\right). \quad (33)$$

For laminar flow, the value of the shear decay coefficient takes a constant value, irrespective of Reynolds Number, Warda et al [7] developed a suitable value as:

$$C^* = 0.0215. \quad (34)$$

By solving the set of equations, from (25) to (34), the MOC model can deal with unsteady friction and the viscoelastic behavior of the pipe walls in transient problems.

Next, the numerical model will be verified against laminar and turbulent flow experimental data to examine its efficiency and accuracy in simulating the pressure transients in viscoelastic pipes.

4.4. Evaluation of the constants for the viscoelastic model

Due to the scarcity of data concerning the viscoelastic behavior of PVC pipes, the data reported by Guney [15] for low-density polyethylene is used as a starting point in the analysis and is afterwards fine tuned to be adjusted for PVC material. The creep compliance curve for low-density polyethylene (LDPE) at 25°C, reported by Guney [15], is shown in fig. 5.

To apply a Kelvin-Voigt Model, the creep compliance curve must be fitted to eq. (28) given by Guney [15] in the form:

$$J(t) = J_o + \sum_{j=1}^{n} J_j\left(1 - e^{-t/\tau_j}\right). \quad (35)$$

Where: $J_o = \frac{1}{E_o}$, and $J_j = \frac{1}{E_j}$.

For a one-element Kelvin-Voigt Model, eq.. (35) could be simplified to:

$$J(t) = J_o + J_1\left(1 - e^{-t/\tau_1}\right). \quad (36)$$

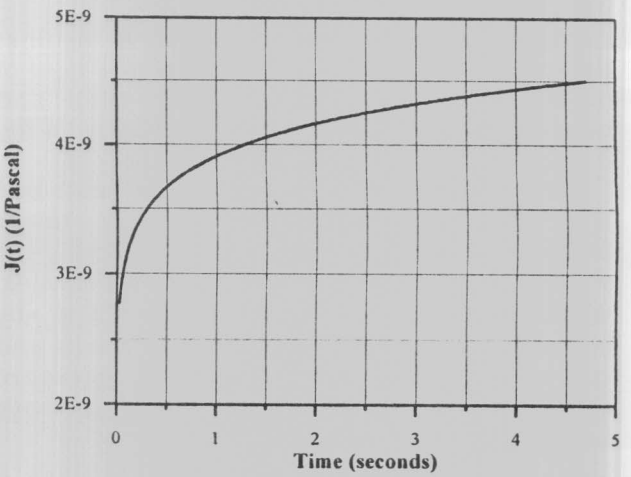

Fig. 5. Creep compliance curve for LDPE at 25°C.

Therefore, by fitting the creep compliance curve using eq. (36), the constants for the viscoelastic model ($E_1=1/J_1$, τ_1) are evaluated. The curve fitting procedure was carried out using a nonlinear correction model. The following results were obtained: E_1=689 MPa, and τ_1 = 0.74 seconds.

These preliminary values are used to simulate a laminar flow case (R_N = 1575). A comparison between the experimental data for this case and the results of the simulation is shown in fig. 6.

From fig. 6, it is noted that, there is no phase shift between the experimental and numerical results, therefore no adjustment is needed for the value of τ_1. Fine tuning is needed for the value of E_1 to adjust the values of the pressure peaks. A value of E_1=1350 MPa provided the best simulation and this is shown in fig. 7.

Therefore, the viscoelastic parameters for the PVC material of the pipe used in the measurements were estimated to be: E_1=1350 MPa, and τ_1= 0.74 seconds.

5. Verification of the viscoelastic model

5.1. Verification of the model for laminar flow

From fig. 7, the viscoelastic model is shown to be capable of accurately modeling transient laminar pipe flow.

5.2. Verification of the model for turbulent flow

The model is further verified against turbulent flow cases. A turbulent flow case of (R_N = 5918) is simulated using the model and the results of the simulation are shown in fig. 8.

Hence, from figs. 7 and 8, it is concluded that a one-element Kelvin-Voigt linear viscoelastic model is capable of predicting the viscoelastic behavior of the pipe walls. Also, when the MOC model is modified by implementing both the viscoelastic model and the unsteady friction model, the pressure transient is effectively simulated for both laminar and turbulent flows.

5.3. Verification at a point along the pipe other than at the valve

In this section, the model is used to simulate the pressure transient at a point 15.3 m upstream of the solenoid valve. This simulation demonstrates the capability of the model in predicting the pressure transient at other points along the pipe. A laminar flow case of (R_N = 597) is considered in this simulation. Results of the simulation are shown in fig. 9.

Fig 9 shows that the model is also capable of accurately simulating the pressure transient at other points along the pipe other than the point directly upstream of the valve.

5.4. Comparison between the effects of the pipe viscoelasticity and the unsteady friction on the damping of pressure oscillations

Fig. 10 shows the results of the simulation of the laminar flow case (R_N = 1575). The simulation was performed once with the standard MOC model, then with the unsteady friction model only, then with the unsteady friction model accompanied by the viscoelastic model. From fig. 10, it is shown that the damping in a pipe exhibiting a viscoelastic behavior is mainly due to the viscoelasticity of the pipe while unsteady friction has a minor effect on the overall damping of the pressure transient.

The previous simulation is repeated for a turbulent flow case (R_N=5918). Results of the simulation are shown in fig. 11. Fig 11 shows that, also for turbulent flows, the damping in a pipe exhibiting a viscoelastic behavior is mainly due to the viscoelasticity of the pipe.

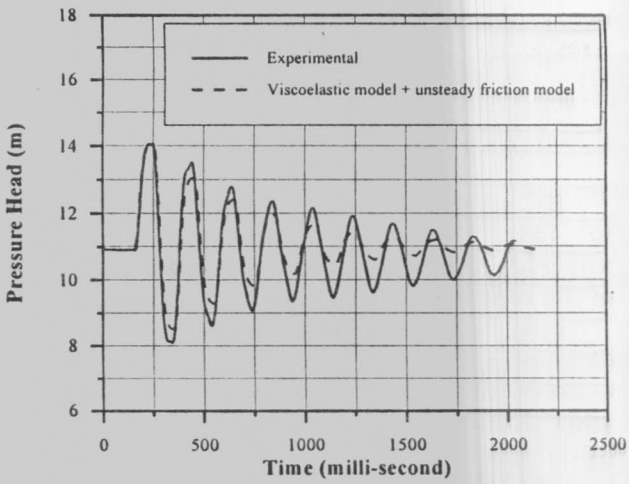

Fig. 6. Viscoelastic model using preliminary values from LDPE, R_N = 1575.

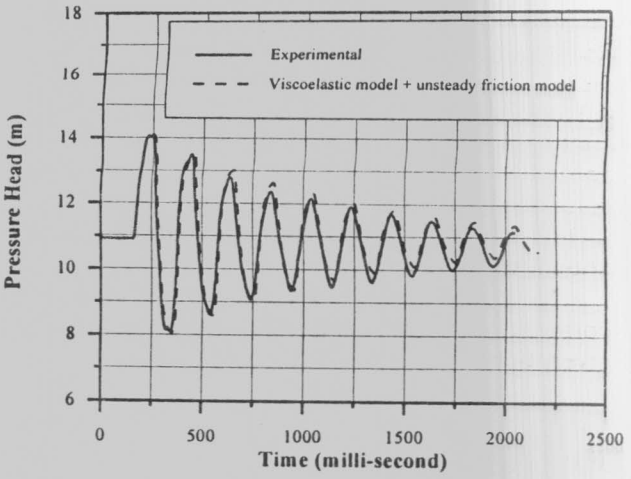

Fig. 7. Viscoelastic model using adjusted values for PVC.

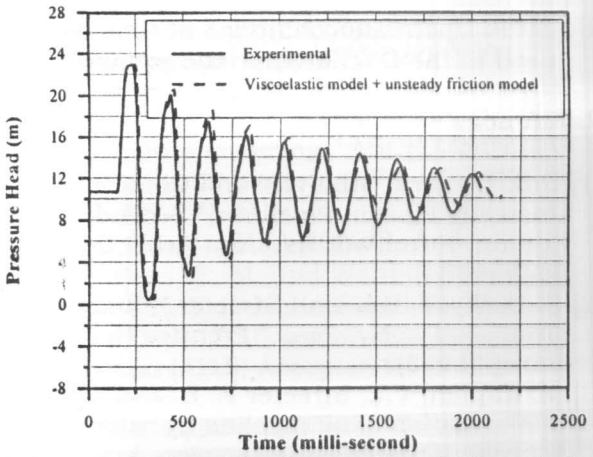

Fig. 8. Verification of the viscoelastic model for turbulent flows.

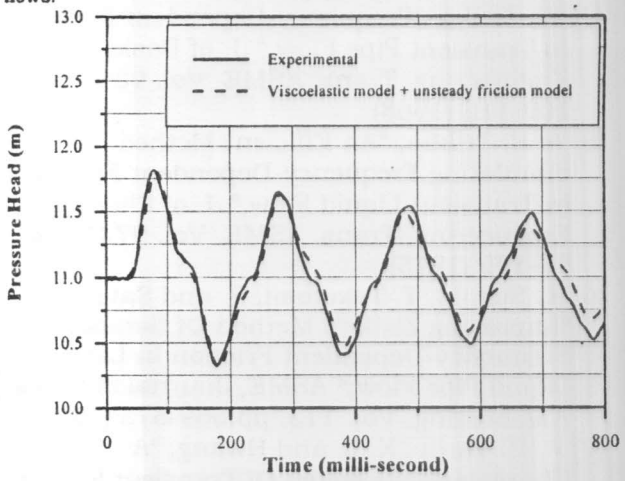

Fig. 9. Verification of the viscoelastic model at a point 15.3m upstream of the solenoid valve, R_N = 597.

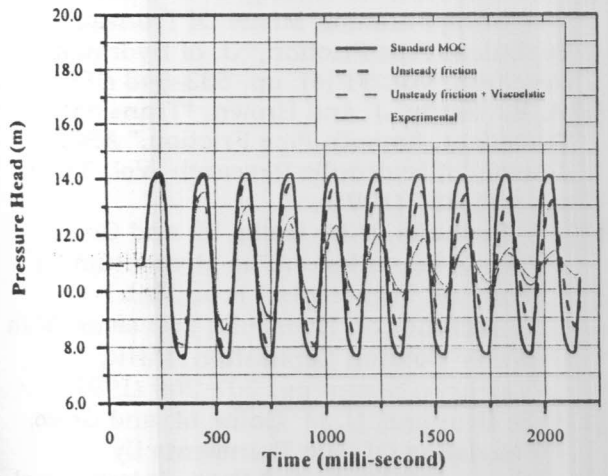

Fig.10. Comparison between the pipe viscoelasticity damping effect and the unsteady friction damping effect.

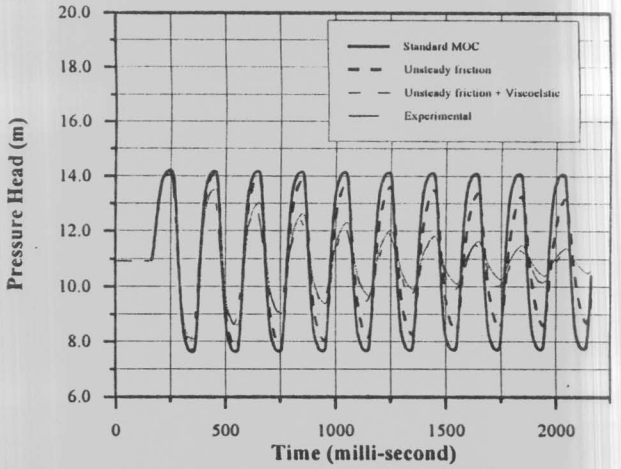

Fig. 11. Comparison between the pipe viscoelasticity damping effect and the unsteady friction damping effect for a turbulent flow case, R_N = 5918.

6. Conclusions

A modified numerical model based on the MOC was developed for modeling pressure transients in a viscoelastic pipeline. The model is capable of dealing with unsteady friction and the viscoelastic behavior of the pipe walls.

1) A one-element Kelvin-Voigt linear viscoelastic model is proved to be capable of accurately predicting the viscoelastic behavior of PVC (plastic) pipes.

2) The results show that the pipe viscoelasticity of viscoelastic pipes is the main cause for the damping of the pressure transient, while unsteady friction has a minor effect on the damping of the pressure transient. This result was obtained for both laminar and turbulent flows.

3) The numerical model is proved to be capable of simulating the pressure transients at points along the pipe other than the point directly upstream of the valve.

4) An efficient method was developed to estimate values for the viscoelastic parameters of PVC, therefore enabling a simple and direct application of the viscoelastic model for any case involving PVC pipes.

Nomenclature

A is the cross-sectional area of the flow, m^2,

a is the wave speed in a fluid in an elastic conduit, m/s,

D is the pipe internal diameter, m,
E is the young's Modulus of Elasticity for the pipe material, N/m^2,
E_j is the modulus of Elasticity of the j^{th} Kelvin-Voigt element, N/m^2,
E is the pipe wall thickness, m,
f is the darcy-Weisbach friction factor,
g is the Gravitational acceleration, m/s^2,
H is the local pressure head, m,
H_b is the barometric pressure head, m,
H_o is the head of the upstream reservoir, m,
$h_f(t)$ is the riction head loss per unit length at time (t), m,
N is the number of pipe segments,
P is the pressure, N/m^2,
Q is the volume flow rate, m^3/s,
R is the pipe radius, m,
R_N is the reynolds number, VD/ν,
t is the time, s,
V is the Mean velocity of the flow, m/s,
V_o is the Steady state mean velocity of the flow, m/s,
s is the Distance along the pipe, m,
z is the node elevation from a reference level, m,
Δt is the Time step size used in the MOC solution,
λ is the Constraint coefficient in the wave speed formula and also used as the multiplier in the Solution by the MOC,
η_j is the viscosity of the generic Kelvin-Voigt element, Ns/m^2,
ν is the kinematic viscosity of the fluid, m^2/s,
ρ is the Fluid density, kg/m^3 ,
τ is the Dimensionless time in the unsteady friction models, ($\tau = \frac{\nu}{R^2} t$), and
$\tau_j = \frac{\eta_j}{E_j}$ is the retardation time of the jth Kelvin-Voigt element, s ,

Subscripts

L is the Downstream conditions at time ($t-\Delta t$) used in the C^- characteristic equation,
P is the Node to be considered at time (t), and
R is the Upstream conditions at time ($t-\Delta t$) used in the C^+ characteristic equation.

References

[1] G.Z. Watters, "Analysis and Control of Unsteady Flow in Pipelines," Second Edition, Butterworths, Ann Arbor Science Book (1984).
[2] E. B. Wylie, V.L. and Streeter "Fluid Transients in Systems," Prentice Hall, New Jersey (1993).
[3] M. Kaplan, V.L. Streeter E. B. and Wylie "Computation of oil pipeline transients," Journal of the Pipeline Division, Proc., ASCE, Vol. 93(PL3) (1967).
[4] W. Zielke, "Frequency-Dependent Friction In Transient Pipe Flow," J. of Basic Engineering, Trans. ASME, Vol. 90 (1), pp. 109-115 (1968).
[5] A. K. Trikha, "An Efficient Method For Simulating Frequency-Dependent Friction In Transient Liquid Flow," J. of Fluids Engineering, Trans. ASME, Vol. 97 (1), pp. 97-105 (1975).
[6] K. Suzuki, T. Taketomi, S. and Sato, "Improving Zielke's Method Of Simulating Frequency-Dependent Friction In Laminar Liquid Pipe Flow," ASME, Journal of Fluids Engineering, Vol. 113, pp.569-573 (1991).
[7] A. E. Vardy, K. L. and Hwang, "A Characteristics Model Of Transient Friction In Pipes," Journal of Hydraulic Research, Vol. 29 (5), pp. 669-684 (1991).
[8] A.E. Vardy, K. L. Hwang, J. and Brown, "A Weighting Function Model Of Transient Turbulent Pipe Friction," J. of Hydraulic Research, Vol. 31 (4), pp. 533-548 (1993).
[9] A. E. Vardy, J. and Brown, "Transient, Turbulent, Smooth Pipe Friction," ASCE, Journal of Hydraulic Research, Vol. 33 (4), pp. 435-456 (1995).
[10] B. Brunone, U.M. Golia, M. and Greco, "Some Remarks on The Momentum Eq For Fast Transients," Proc., Int. Conference on Hydraulic Transients With Water Column Separation, IAHR, Valencia, Spain, pp. 201-209 (1991).
[11] B. Brunone, U. M. Golia, M. and Greco, "Modeling Of Fast Transients By Numerical Methods," Proc., International Conference On Hydraulic Transients

With Water Column Separation, IAHR, Valencia, Spain, pp. 273-280 (1991).

[12] B. Brunone, U. M. Golia, and Greco, M., "Effects Of Two-Dimensionality On Pipe Transients Modeling," ASCE, Journal of Hydraulic Engineering, Vol. 121 (12), pp. 906-912 (1995).

[13] H. A. Warda, H. A. Kandil, A. A. Elmiligui, E. M. and Wahba, "Modeling Unsteady Friction in Rapid Transient Pipe Flows ," Alexandria Engineering Journal (AEJ), Accepted for publication (2001).

[14] L. Suo, E. B. and Wylie, "Complex Wave Speed And Hydraulic Transients In Viscoelastic Pipes," J. of Fluids Engineering, Trans. ASME, Vol. 112, pp. 496-500 (1990).

[15] M. S. Guney, "Waterhammer In Viscoelastic Pipes Where Cross-Section Parameters Are Time Dependent," Proc., 4th Int. Conference on Pressure Surges, British Hydromechanics Research Association (BHRA), Cranfield, U.K., pp. 189-204 (1983).

[16] G. Pezzinga, P. and Scandura, "Unsteady Flow In Installations With Polymeric Additional Pipe," ASCE, Journal of Hydraulic Engineering, Vol. 121 (11), pp. 802-811 (1995).

Received July 11, 2001
Accepted October 25, 2001